

# Improving the Stepped Distiller Performance in Combination with Vertical Corrugated Wick Solar Still and Finned Absorber

A. Aldabesh\*

Department of Mechanical Engineering, Faculty of Engineering, Al-Baha University, 65799, Al-Baha, Saudi Arabia

Received 8 June 2025

Accepted 8 October 2025

## Abstract

This work studied a new advancement in solar distillation that combines altered modified stepped solar stills (STSSs) with 3 novel features: STSS with vertical corrugated wick SS (MSTSS-VCWSS), MSTSS with finned wick absorber (MSTSS-FWA) and paraffin wax containing silver nanoparticles (PCM-Ag-NPs). The rising water issue caused by population increase and loss of freshwater resources was the driving force behind the research. According to experimental data, the highest freshwater production was obtained for MSTSS-FWA with VCWSS and PCMs-Ag, where the combined productivity of the MSTSS-FWA+VCWSS+ PCMs-Ag reached 11950 ml/m<sup>2</sup>/d, representing a substantial 273% increase over conventional SS. Water costs \$0.028 per litre for CSS and \$0.011 per liter for MSTSS-FWA+VCWSS+ PCMs-Ag.

© 2025 Jordan Journal of Mechanical and Industrial Engineering. All rights reserved

**Keywords:** Sustainability; Vertical wick distiller; Stepped distiller; Finned solar stills; Solar desalinization.

## Nomenclature

Symbol	Description
$\eta_{th}$	Thermal efficiency
A	Area
Ag-Nano	Silver nanomaterial
CPL	Distilled water cost, \$
F	Fixed costs, \$
$h_{fg}$	Latent heat
i	Interest rate, %
I	Sun irradiation
m	Distillate
MSTSS-FA	Modified stepped SS with finned absorber
MSTSS-FA-	Modified stepped SS with finned absorber,
PCM-Ag-EF	PCMS-Ag.
n	Lifespan
N	Operational time
PCM	Phase change material
STSS	Stepped solar still
S	Salvage value, \$
SFF	Sinking fund factor
VCWSS	Vertical corrugated wick solar still
AMC	Annual maintaining expenses, \$
ASV	Annual salvage value, \$
CRP	Capital recovery parameter
TAC	Accumulative yearly costs, \$
$\eta_{th}$	Thermal efficiency

## 1. Introduction

The global challenge of scarce water resources has spurred broad exploration into effective desalination methods. Whilst traditional techniques be, their economic practicality is a hindrance [1]. As a result, scientists have looked on substitute techniques, and solar distillation has

emerged as a viable one [2]. Harnessing sun energy for drinkable water presents a sustained and non-conventional scheme [3]. Worldwide, scholars designed, built, and assessed numerous distiller configurations, including traditional and enhanced designs. Results offered powerful insights to the readers. Particularly, passive solar desalination has been extensively studied for optimal performance. Despite the existence of accomplished techniques as multi-effect desalination [4], renowned for being expensive and difficult [5], conventional solar stills (CSS) offer a simpler and more economical approach. Nevertheless, a literature highlights efficiency limitations in current designs.

CSSs are highly engaging owing to cost-effectiveness, simplicity, and use of favorable materials. Nevertheless, their yield is low 3 liters with efficacy of around 30%. Scientists proposed versatile adjustments to overcome restrictions and improve the CSS efficacy. To tackle restrictions, scientists explored numerous designable shapes such as trays [6], dishes [7], , stepped [8], wick [9], tubular [10], semispherical [11], & pyramidal [12] patterns. This approach aims to promote vaporization and subsequently heighten yield. Moreover, integrating different liner forms [13] and calcium hydroxide coating [14].

Researchers explored different patterns of stepped distiller as inclined vacuum-insulated versions. Zhang et al. [15] conducted the effectiveness of a modified stepped SS, freshwater production increased significantly to 3300 mL/m<sup>2</sup>/day. representing a 1.4-fold improvement over CSS. Similarly, Lashgari et al. [16] observed enhancements in output with a six-stage STSS, achieving a remarkable 4700

\* Corresponding author e-mail: dr.algabesh@bu.edu.sa.

mL/m<sup>2</sup>.day, which is 2.5 times more than that of CSS. STSS achieve higher efficiency levels primarily due to their intricate design [17]. Works have investigated the incorporation of PCMs within the heat exchangers of these stills [18]. While PCM integration has demonstrated improvements in efficacy by increasing heat transfer and minimizing heat loss, it also introduces added complexity and cost to system. El-Sebaey et al. [19] created steps inside a tubular SS to enhance its performance. They obtained 49.29% improve in production. There are also many studies concerning with water desalination and demonstrating the different performance of distillates [20-22].

An article by Azizi et al. [23] investigated ways to increase the PVT (photovoltaic thermal) unit's production when dust is present. In order to increase electrical production, this study focuses on a PVT system that consists of a cooling tube with anchor-shaped fins and photovoltaic (PV) cells integrated with thermoelectric generator (TEG) modules. A hybrid nanofluid made of water and Fe<sub>3</sub>O<sub>4</sub>/SiO<sub>2</sub> nanoparticles is used inside the cooling tube to maximize system performance in dusty environments. To lessen the effect of dust deposition, SiO<sub>2</sub> nanoparticles are also applied to the glass layer as part of a self-cleaning approach. The findings shown that adding fins and increasing the hybrid nanofluid's velocity improves temperature uniformity throughout the panel when there is no dust present.

An external investigation was carried out by kushwahet al. [24] for both an advanced solar still and a traditional SS. A water heating coil, an external condenser, and Nano-PCM (ZnO-PCM) were among the modifications used to increase the advanced SS' production. The findings showed that the advanced solar still with a heating coil had a 46% thermal efficiency and a 77% improvement in production, the advanced solar still with an external condenser had a 53% thermal efficiency and a 119% yield improvement, and the advanced SS with ZnO-PCM had a 51% efficacy and a 113% improvement in production. With ZnO-PCM, the advanced solar still's production increased by around 36%, and with an exterior condenser. The cost of desalinated freshwater, according to economic analysis, was \$0.021 per liter for the modified solar still with an exterior condenser, \$0.023 per liter for the modified SS with ZnO-PCM, and \$0.030 per liter for the conventional SS.

The research aims to increase the yield of stepped distiller (STSS) by adding vertical corrugated wicking distiller (VCWSS) behind it. So, we benefit from warm wastewater resulting from VCWSS to flow stepped SS. The VCWSS does not occupy horizontal space, as the width of the still is only 10 cm. Therefore, a glass was established on back wall where the steam is condensed on it. Condensation occurs on the front and back surfaces of the VCWSS. In this study, 3 modifications were made to the stepped SS as

following: (a) The VCWSS is fed from feeding reservoir and the feed water enters a horizontal pipe perforated at distiller top. The hot waste water from VCWSS enters as feed water to stepped SS. There is a second feed to stepped SS from the change tank directly, (b) the second modification is to add a finned base covered with wick to increase the surface area of stepped SS base and reduce the amount of water in the base. The third modification is adding PCM-Ag under the base of the STSS, to lessen the glass temperature of the STSS.

## 2. Methodology

### 2.1. Setup fabrication

Fig. 1 illustrates a photo of actual setup, whilst Fig. 2 presents a 2-D schematic of system. The conventional single-basin solar still (CSS) described here is designed with specific materials and features to optimize its performance. The use of 0.15 cm thickness galvanized steel sheet for construction ensures durability and longevity. The dimensions of the still, (49.5 cm × 50 cm × 15 cm), are chosen to balance water volume and solar exposure. The addition of a 3 mm glass cover fixed on a steel frame serves multiple purposes. It acts as a condensing surface, collecting condensed water droplets and channeling them to the collecting trough. The glass cover's inclination angle (32°) likely aids in directing the condensed water efficiently. To minimize heat losses, insulation of fiberglass is applied to the exterior surfaces of the solar still. This insulation helps maintain a stable internal temperature conducive to efficient distillation. The freshwater collection system, comprising a flexible hose and calibrated flask connected to the inclined trough, allows for easy and accurate measurement of distilled water output. The STSS maintains the same dimensions and construction as the CSS. However, it incorporates an absorber plate with five steps, each measuring 10 cm x 100 cm. This design, illustrated in Fig. 2, increases the surface area available for evaporations and condensation, enhancing the distillation efficiency of the system.

The vertical wick's capillary-driven hydration enables accelerated evaporation kinetics, while its compact geometry (1 m length × 0.1 m width × 1 m height) optimizes land-use efficiency. To mitigate radiative heat loss from the wick-obstructed rear wall, a supplementary glass condensation panel was installed on the posterior surface, enabling dual-side condensation (anterior and posterior glazing). Furthermore, the wick was mounted on a corrugated structural profile to maximize irradiated wick surface area, thereby enhancing evaporation rates. The system employs a closed-loop feed mechanism: a low-capacity pump delivers feedwater from the reservoir to a perforated distribution manifold at the vertical still's apex.



a. Conventional solar still



b. Stepped SS with vertical corrugated wick still

Figure 1. Experimental tested SSs

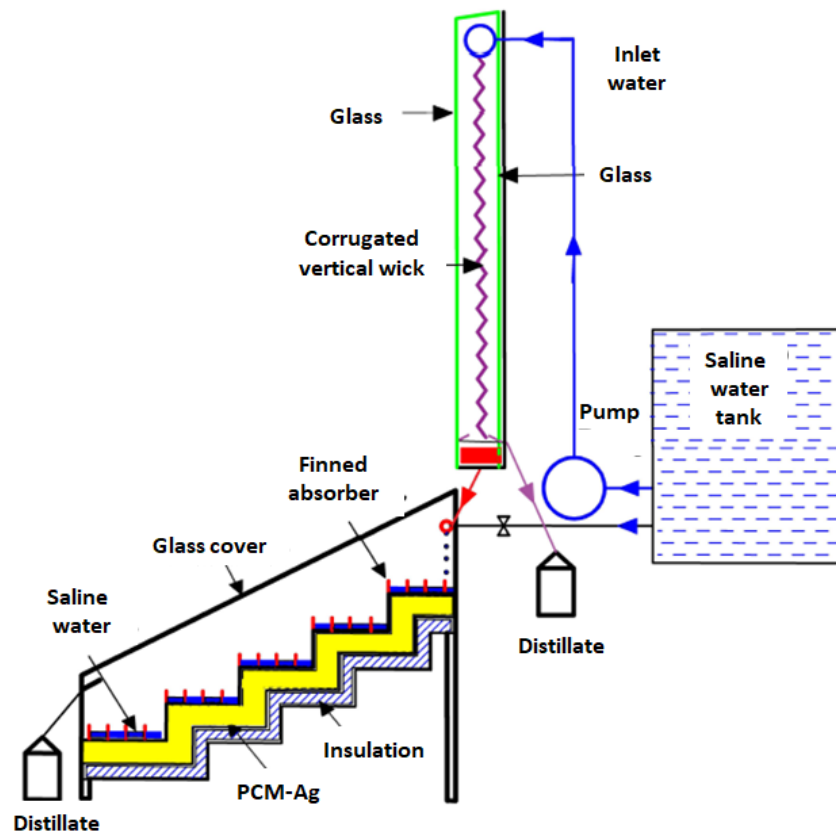


Figure 2. Scheme of test-rig.

Energy-efficient SSs are designed to maximize the utilization of solar energy for the distillation process. While heat dissipation from the condenser glass cover is crucial for facilitating the rapid and complete condensation of water vapor, thermal losses from the base and sidewalls represent inefficiencies that can be minimized. It is possible to mitigate these losses significantly, thereby increasing overall thermal efficacy to approximately 60%. A prominent strategy involves capturing the surplus thermal energy

available through peak solar hours, as well as recovering lost heat from the structural components, using a PCM. This stored latent heat can subsequently be discharged during off-sun hours (evening and night) to sustain the distillation process, effectively allowing the PCM to function as an auxiliary heat source.

Among various nanomaterials investigated for enhancing PCM thermal conductivity, copper oxide (CuO) nanoparticles have been identified as particularly effective

when blended with paraffin wax. However, recent research has explored even more suitable alternatives. Silver (Ag) nanoparticles, for instance, possess a superior intrinsic TC (thermal conductivity) (419 W/m·K) compared to CuO (76.5 W/m·K) or TiO<sub>2</sub> (4.8 W/m·K). This property makes them excellent candidates for nanocomposite PCMs.

In the present study, high-purity (99.2%) silver nano powder was integrated into paraffin wax at 2.5% mass fraction of (975 g PCM + 25 g Nano-Ag) to address its inherently low TC. The Nano composite (PCM-Ag) was prepared by first melting the paraffin wax at 60°C. The Ag nanoparticles were then gradually introduced under continuous magnetic stirring for one hour. To ensure a homogeneous dispersion and prevent nanoparticle agglomeration, the mixture was subsequently subjected to ultrasonic vibration for two hours. The thermophysical properties of the base PCM and the resulting Nano-PCM are detailed in Table 1. Nano silver was purchased from the market.

**Table 1.** The thermophysical properties of paraffin wax both with and without silver Nano.

Property	Ag- Nano + PCM	PCM	Units
Density	962	876	kg/m <sup>3</sup>
Latent heat of fusion	182	190	kJ/kg °C
Melting point	53	54.5	°C
Specific heat	2.01	2.1	kJ/kg °C
Thermal conductivity	0.3	0.21	W/m °C

The inclusion of Ag nanoparticles significantly altered the thermal characteristics of the paraffin wax. The thermal conductivity increases proportionally with the nanoparticle concentration up to an optimal point of 2.5 wt.%, beyond which it stabilizes. This informed the concentration selection for this study. The measured thermal conductivity improved from approximately 0.21 for pure paraffin wax to 0.30 W/m·°C for the Ag-based Nano-PCMs. This enhancement shortens the charging (melting) time of the PCM. Furthermore, results indicate a depression in the phase change temperatures, with the melting and solidification points decreasing from about 54.5°C to 53°C. This reduction, coupled with an increased heat release rate, accelerates the discharging (solidification) processes. The overall effect is a more efficient thermal storage system that elevates water temperature, accelerates evaporation rates, and thus enhances the solar still's productivity compared to systems employing non-enhanced PCM. The pump is used

to raise water from the tank to the pipe of the wick distiller, and the working periods range from 30 seconds to 90 seconds every hour, depending on the degree of wetness of the wick. (Water pump motor AC motor, 220 V, 10 W, 1.3 L/min).

Type K thermocouples were all employed in the experiment. There are five steps and ten water thermocouples in the stepped still basin, and two thermocouples were positioned 25 cm from each side of the stairs to measure the water's temperature. The water temperature in the basin was calculated by averaging these ten measurements. Two thermocouples were positioned 25 cm from either side of the glass cover, and measurements were made at two positions in the middle of the cover to determine the temperature of the glass surface. Two points along the vertical axis of the vertical wick distiller were used to record the wick temperature: one was 25 cm from the bottom, and the other was 25 cm from the top, close to the middle. The wick temperature was calculated by averaging these two measurements. In a similar manner, two locations precisely opposite the wick measurement places were utilized to measure the temperature of the front glass, and the average of these readings was used. Ten places that corresponded to the water temperature points in the base were used to measure the wax temperature for the modified stepped distiller. The wax temperature was represented by the average of these, which were measured 1 cm above the bottom surface.

## 2.2. Uncertainty Analysis

An uncertainty analysis was conducted to quantify the reliability of the experimental measurements and the reported results. The uncertainties associated with the direct measurements are provided by the instrument manufacturers and calibration certificates. The overall uncertainty in the calculated parameters, such as daily productivity and thermal efficiency, was determined using the root-sum-square (RSS) method for error propagation [25].

The general form of the RSS equation for a dependent result  $R$ , which is a function of  $n$  independent variables  $x_1, x_2, \dots, x_n$ , is given by:

$$U_R = \sqrt{\left(\frac{\partial R}{\partial x_1} U_{x_1}\right)^2 + \left(\frac{\partial R}{\partial x_2} U_{x_2}\right)^2 + \dots + \left(\frac{\partial R}{\partial x_n} U_{x_n}\right)^2} \quad (1)$$

where  $U_R$  is the total uncertainty of the result and  $U_{x_1}, U_{x_2}, \dots, U_{x_n}$  are the uncertainties of the independent variables.

Table 2 below provides a summary of the key measuring instruments' uncertainties.

**Table 2.** Accuracies and uncertainties of measuring instruments

Instrument	Measured Parameter	Range	Accuracy	Uncertainty	Units
K-type Thermocouples	Temperature	0–100	±0.5	±0.5	°C
Pyranometer (Kipp&Zonen SP Lite2)	Solar Irradiance	0–2000	±5%	±50 (at 1000)	W/m <sup>2</sup>
Graduated Flask (Class A)	Freshwater Yield	0–1000	±1	±1	mL
Thermal Anemometer (Testo 405i)	Air Velocity	0–20	±0.1	±0.1	m/s

### 3. Results and discussion

#### 3.1. Performance of stepped SS & traditional SS

From Fig. 3, it is shown that glass temperatures and water temperatures of STSS are slightly greater than those of traditional SS by approximately 0.2 °C and 0.3 °C, severally. The STSS exhibited consistently greater water temperatures (by 0 - 3 °C) compared to conventional SS. This temperature difference translates to a greater evaporation rate and consequently, increased productivity for the stepped SS. A similar trend is observed for condensation rate, as evidenced by the higher glass temperatures (by 0 to 2 °C) in the stepped SS. Despite these modest temperature variations and the presence of a small air pocket within the STSS due to its design, the stepped SS achieved a 30% improvement in distillation over CSS. This is reflected in efficiency values, with the STSS reaching 38.5% efficiency compared to the CSS's 34%. Additionally, the glazing temperature of STSS and CSS were 46.5 and 44.5 °C at 13:00. While, the water temperature of stepped SS and CSS were 65 and 63 °C at 13:00. This observation can be attributed to 2 main reasons: Firstly, the stepped SS has a smaller air volume trapped inside the still chamber compared to the traditional still, leading to faster heating of the trapped air. Secondly, the steps design of the basin in the stepped SS provides a larger heat and mass transfer surface area compared to the flat basin of the CSS, thereby resulting in an increase in water temperature of basin of the STSS. Additionally, the higher water temperature contributes to an increased evaporations and condensations rates, consequently leading to a rise in the glass temperatures of the stepped distiller. The irradiation at 12:00 PM is 1080 W/m<sup>2</sup> and ambient temperature is 40.5 °C.

Because of the greatest temperature differential between the glass plate and the wick material, the optimal time frame for producing the most distilled water was determined to be between 11:00 am and 3:30 pm. It is evident from Fig. 3 that the distillation and sunradiation curve behave more similarly than the wind velocity curve. As a result, productivity is more dependent on solar radiation than wind speed. Fig. 3 indicates the hourly variation of suncurve with time of the day. It can be noted that, the sun radiation increased with increasing time till a maximum value at noon and thereafter started to decrease. The sun radiation over SS is about 700 at 9:00 am, 1080 at 12 pm and 85 W/m<sup>2</sup> at 6 pm.

The analysis reveals that the accumulated distillate volume for the STSS is greater than that of the CSS, Fig. 1, with the hourly freshwater productivity be notably higher for the stepped solar still. Specifically, the daily total productivity reaches approximately 4150 ml/m<sup>2</sup> for stepped SS and 3200 ml/m<sup>2</sup> for conventional SS. Consequently, the increase in stepped SS distillate is approximately 30% over than that of traditional SS in this scenario.

As anticipated, the afternoon saw the highest productivity, while the morning, when the water had not yet heated up, saw the least amount of distilled water. A high ambient temperature (Fig. 3) and high insolation heating (Fig. 4) would cause this increase in water productivity. Moreover, the water supplied to the system in the early morning has a low temperature and requires time to warm up. Steppes are used to expand the brine's evaporating

surface area through the solar still's base and vertical walls. Furthermore, compared to CSS, it gives the still a low thermal capacity and, as a result, responds to incident solar radiation more quickly, raising the temperature of the brine water and producing higher evaporation rates.

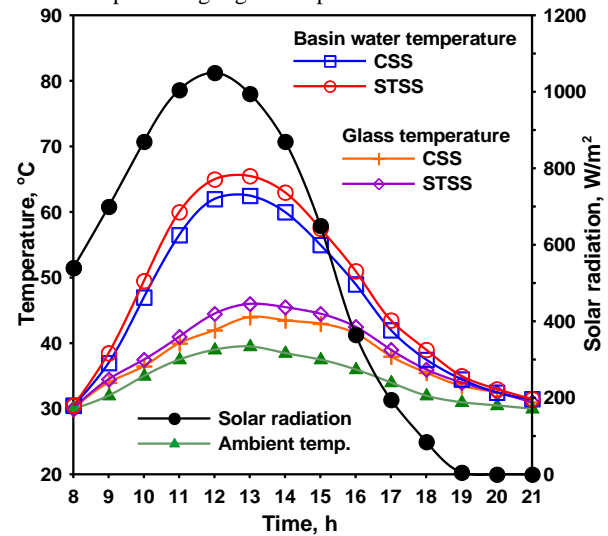


Figure 3. Solar irradiation and temperatures of ambient, water and glass for both distillers.

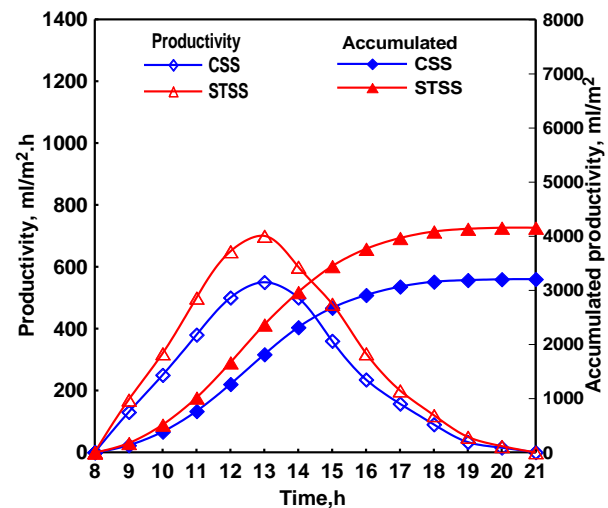


Figure 2. The variations of yields for CSS & STSS

#### 3.2. Performance of stepped SS with VCWSS (MSTSS)

After adding VCWSS to STSS, the modified stepped still is abbreviated by MSTSS. The results illustrate the variations in irradiance and the temperatures of air, fluid, and glazing for CSS & MSTSS. The feeding water temperature for conventional SS was occasionally marginally bigger than air temperature, and at times, it was nearly equal, influenced by external atmospheric condition. While MSTSS received feed water from two sources: VCWSS and feeding tank, ensuring coherent water leveling. The water from VCWSS was consistently 0.5-6.5 °C warmer over air temperature. Consequently, MSTSS's water temperature was consistently higher than conventional SS's, ranging from 0 to 5.5 °C. Water temperature of MSTSS was 68.5 °C, while conventional SS temperature of water was 63 °C, at 13:00. This temperature difference led to higher evaporation rates in MSTSS, resulting in a higher glass

temperature compared to the conventional SS, ranging from 0 to 5.5 °C. Glass temperature of MSTSS was 50.5°C, and conventional SS glazing temperature was 45°C, at 13:00,. Additionally, at 12:00, the irradiation was 1190 W/m<sup>2</sup>, and the air temperature of was 41.5°C.

Fig. 5 illustrates the productivity changes for CSS, modified stepped SS, VCWSS, & cumulative output of modified stepped SS & VCWSS. Modified stepped TSS consistently outperformed CSS & VCWSS for output due to its higher water temperature and evaporation rate. At 13:00, the freshwater productivity reached 930 ml/m<sup>2</sup> for modified stepped SS, 500 for the VCWSS, and 600 ml/m<sup>2</sup> for CSS. Consequently, the total daily productivity was 5900 for MSTSS, 3350 ml/m<sup>2</sup> for CSS, and 3600 ml/m<sup>2</sup> for VCWSS. This represents a 74.6% output improvement for modified stepped SS over CSS. In addition, the total combined productivity of the VCWSS and MSTSS together reached 9500 ml/m<sup>2</sup>/day, so the percentage increase in productivity in this case was 183.5% over the conventional SS.

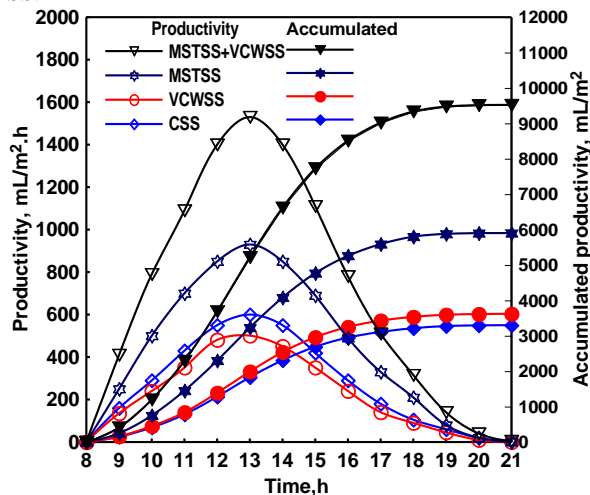


**Figure 5.** Variations of production for conventional SS, modified stepped SS and VCWSS & cumulative yields of modified stepped SS & VCWSS.

### 3.3. Performance of modified stepped SS with finned absorbers (modified stepped SS-FWA)

The second modification is the addition of a corrugated base covered with wick to increase the surface area of modified stepped SS base and reduce the amount of water in the base. The modified stepped SS with finned absorber is abbreviated by modified stepped SS-FWA. Also, the amount of water is less by about 50%, as the amount of water with modified stepped SS-FWA is 4.5 L, while the CSS water amount is 5 L. Thus, the temperature of water of the modified stepped SS-FWA rises at a faster rate. Also, the wick over the absorber surface gets wet by capillary action. The optimal water volume is achieved when no water rises inside the tray, ensuring the wick remains only moist. This condition is met with a water volume of 1.5 liters; however, practical application is not feasible due to the wick on the slant being supplied by the small amount of water with finned board. Additionally, the withdrawal rate varies hourly based on radiation intensity. Consequently, a volume of 4.5 liters was selected to ensure continuous self-feeding of water in the tray, preventing dry spots and maintaining consistent productivity.

Comparing the basin water temperature of the MSTSS-FWA and the CSS, it is showed that the basin water temperatures for MSTSS-FWA are approximately 0 to 9 °C greater than those for conventional SS. Furthermore, the top water temperatures recorded are 64 °C for CSS and 73 °C for modified stepped SS-FWA, happening at 13:00. Likewise, the glazing temperature for modified stepped SS-FWA was about 0 to 7.5 °C higher than those for conventional SS, with the highest glass cover temperatures being 44.5 °C for CSS and 52 °C for modified stepped SS-FWA, also at 13:00. These variations are due to differences in water mass within distiller and the respective surface areas exposed to irradiation. Also, at 12:00 the measurements indicate that the maximum sun energy recorded through the day is 1100 W/m<sup>2</sup>.

The increase in productivity observed in the modified stepped SS-FWA compared to the conventional SS is attributed to several factors. Firstly, the higher water temperature in MSTSS-FWA contributes to increased evaporation rates. Additionally, modified stepped SS-FWA has a larger exposed area to solar energy. This larger exposed area further enhances evaporation and distillation rates. Moreover, the lower volume of water contained in modified stepped SS-FWA (4.5 L) compared to conventional SS (5 L) leads to faster heating and consequently higher productivity. These combined factors result in the MSTSS-FWA demonstrating higher performance than conventional SS in terms of freshwater production.

The accumulative outputs for CSS, VCWSS, & modified stepped SS-FWA are 3200, 3600, and 7300 mL/m<sup>2</sup>, respectively. This indicates that the modified stepped SS-FWA exhibits approximately a 128% higher cumulative productivity compared to conventional SS. Furthermore, when accounting the cumulative yield of VCWSS & modified stepped SS-FWA together, which totals 10900 mL/m<sup>2</sup>, the yield improvement over conventional SS is 240%.

### 3.4. Performance of MSTSS-CA with VCWSS and PCM-Ag-Nano

The third modification is adding PCM with Ag under the base of the STSS, and this is the result of feeding hot water coming from the VCWSS to the STSS, the temperatures of the water for the STSS increases, the evaporations rate increases, and the temperature of the glass of the STSS rises, especially during the period of intense radiation, so improved paraffin wax mixed with Ag-Nanos was used. Fig. 6 depicts the variations in water temperature observed in both distillation units, namely the CSS and the MSTSS-FWA, along with the temperature profile of PCM-Ag-NPs within MSTSS-FWA. Through initial phase, the water temperatures within conventional SS register a marginally higher level (by 0 to 1 °C) over MSTSS-FWA. This discrepancy in temperature is ascribed to the intrinsic heat absorption capabilities of PCM integrated within MSTSS-FWA. As PCM undergoes the phase transition to its liquid state during the charging process, it actively absorbs heat from the surrounding water within MSTSS-FWA, leading to a transient decline in water temperature. Importantly, by midday, a convergence in water temperatures between the two stills is discernible, indicating a potential saturation of



phase change material's thermal energy absorption capacity at this juncture. The integration of PCM-Ag-NPs into MSTSS-FWA led to a slight reduction in the glass temperatures when compared to MSTSS-FWA lacking this composite material.

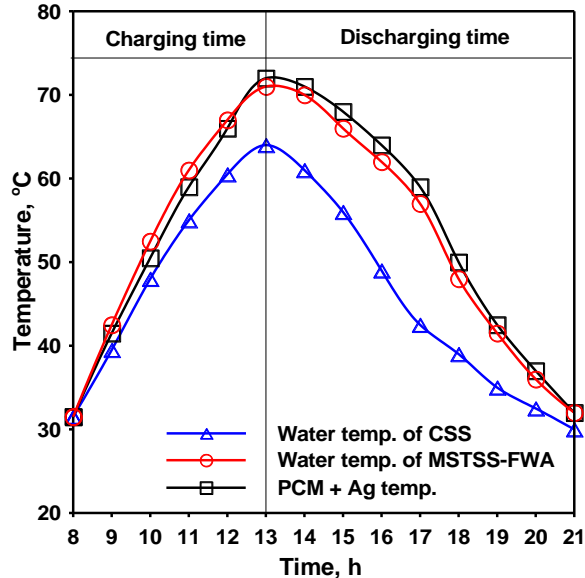


Figure 6. Water and PCMs temperature inside MSTSS.

The results indicated that real-time variations in freshwater yields observed in the CSS, MSTSS-FWA, VCWSS, and the combined MSTSS-FWA and vertical wick SS when incorporating PCMs-Ag-Nanos. During the initial phase of the experiment (before noon), it was noted that the traditional SS exhibited a greater productivity compared to the MSTSS-FWA. This disparity can be ascribed to the lower temperature of water in the MSTSS-FWA resulting from the heat absorption characteristics of the integrated PCMs-Ag-Nanos composite. However, this trend underwent a reversal post-noon. The productivity of MSTSS-FWA began to ascend, surpassing that of CSS. This leads to a total daily productivity of 3200, 7200, and 3600 ml for traditional SS, MSTSS-FWA, & vertical wick SS, severally.

Additionally, the results indicated that MSTSS-FWA (8350 mL/m<sup>2</sup>.day) achieved a notable 161% increase in productivity when compared to CSS (3200 mL/m<sup>2</sup>.day). Furthermore, through the process of isolating the influence

of PCM-Ag-NPs, it can be estimated that PCM-Ag-NPs contributed to a 33% enhancement in productivity, solely credited to PCM-Ag-NPs. In summary, the cumulative productivity of MSTSS-FWA and VCWSS reached 11950 ml (8350+3600), representing substantial 273% increase over CSS. Table 3 summarizing key findings in a comparative for quick reference.

### 3.5. Efficacy of solar stills

The thermal efficacy ( $\eta$ ) can be determined through the relationship:

$$\eta_d, \% = \frac{\sum \dot{m} \times h_{fg}}{\sum A \times I + \sum \text{External power}} \times 100 \quad (2)$$

The productivity increase can be determined through the relationship,

$$\text{Daily productivity rise, \%} = \frac{\text{Improved Production} - \text{Baseline production}}{\text{Baseline production}} \times 100 \quad (3)$$

The results in Table 3 demonstrate conclusively that the STSS configuration outperforms the CSS in both freshwater thermal efficiency and productivity rise. The baseline CSS exhibited a thermal efficiency of approximately 34.5%. In contrast, the STSS achieved a 30% increase in freshwater yield compared to the reference CSS, along with an efficacy of 39%. Further integration of the VCWSS with the MSTSS-FWA led to a 240% improvement in productivity over baseline levels, accompanied by a thermal efficiency of 68%. The most notable performance enhancement was observed with the incorporation of PCM-Nano, which resulted in a 273% rises in productivity and a corresponding thermal efficacy of 71%.

### 3.6. Economic analysis

To evaluate the STSS system's economic feasibility and practicality, cost calculations were carried out methodically use the economic evaluation equations described in combination with the thorough data shown in Table 4 and the financial assessments presented in Table 5. The studied solar SSs systems have been analyzed to estimate the cost of fresh water produced by reference and stepped SSs. The analysis equations can be showed below [26]:

Table 3. Efficacy and distillate improvement of STSS over CSS.

Solar still type	STSS	ST SS+VCWSS	STSS+VCWSS-FWA	STSS+VCWSS-FWA+PCM-Ag	CSS
Production rise	30%	183.5%	240%	273%	-
Efficiency	39	59.5	68	71	34.5%

The CRF (capital recovery factor) is:

$$CRF = \frac{i(1+i)^n}{(1+i)^n - 1} \quad (4)$$

Where, “ $i$ ” is the interest rate and  $n$  is the life time (years),.

The FAC (fixed annual cost) is:

$$FAC = P (CRF) \quad (5)$$

Where, the capital cost of SS is  $P$  (\$)

The  $SFF$ (sinking fund factor) is:

$$SFF = \frac{i}{(1+i)^n - 1} \quad (6)$$

The  $S$ (salvage value) is:

$$S = 0.2 P \quad (7)$$

The annual salvage value ( $ASV$ ) is:

$$ASV = S (SFF) \quad (8)$$

The annual maintenance and operating costs ( $AMC$ )

$$AMC = 0.15 (FAC) \quad (9)$$

The total annual cost ( $TAC$ )

$$TAC = FAC + AMC - ASV \quad (1)$$

The  $CPL$  (cost of fresh water) in \$ per liter is

$$CPL = TAC / M \quad (2)$$

Where, the average yearly distillate yield is  $M$ .

Consequently, the expenses of desalinated water were \$0.028 per liter for conventional SS and \$0.011 per liter for MSTSS-FWA+VCWSS+PCMs-Ag. The finding underscore the economic advantages of the improvements made to the distillation systems, with the modified stepped SS-FWA reduced expenses over conventional SS.

**Table 4.** Fixed costs of SSs components.

Item	Cost of conventional SS (\$)	Cost of modified stepped SS (\$)
Glass cover	15	30
Iron sheet	20	40
Production	25	40
Ducts and fittings	20	30
Water tank	15	15
Insulation	10	10
Paint	5	5
Pump	-	10
PCM	-	5
Ag-Nano	-	25
<b>Total fixed cost (F)</b>	<b>110</b>	<b>170</b> for MSTSS+VCWSS <b>190</b> for MSTSS-FWA+VCWSS <b>210</b> for MSTSS-FWA+VCWSS+PCMs-Ag

**Table 5.** Assumptions used in the economic analysis.

No.	Variable	Mean	Quantity	Unit
1.	$n$	Lifetime of the system	20	Years
2.	$N$	Days of the year that work	340	Day
3.	$i$	Interest rate	15	%
4.	$F$	Fixed cost of system	150 for MSTSS+VCWSS	\$
			190 for MSTSS-FWA+VCWSS	
			220 for MSTSS-FWA+VCWSS+PCMs-Ag	
			110 for CSS	
5.	$M$	Average yearly production	3050 for MSTSS+VCWSS	L/m <sup>2</sup> .year
			3700 for MSTSS-FWA+VCWSS	
			4050 for MSTSS-FWA+VCWSS+PCMs-Ag	
			1080 for CSS	
6.	CPL	Distilled water cost	0.012 for MSTSS+VCWSS	\$/L
			0.0113 for MSTSS-FWA+VCWSS	
			0.011 for MSTSS-FWA+VCWSS+PCMs-Ag	
			0.028 for CSS	



#### 4. Conclusions and future work

This paper aims to increase the production of the stepped solar stills (STSSs) by adding a vertical wick distiller (VCWSS) behind it. The second modification is to add a corrugated base covered with wick to improve the surface area of modified stepped SS base and reduce the amount of water in the base. Also, the effect of adding paraffin wax with nanomaterials under the STSS base is investigated. Key findings of the study include:

1. The daily productivity of CSS and modified stepped SS was 3200 and 4150 ml/m<sup>2</sup>/day. Consequently, the increase in STSS freshwater is approximately 30% higher than that of CSS.
2. The yield for conventional SS and modified stepped SS (modified stepped SS+VCWSS) was 3350 and 9500 ml/m<sup>2</sup>/day. Thus, the percentage increase in productivity in this case was 183.5% over the CSS.
3. The yield for CSS and modified stepped SS (modified stepped SS+VCWSS-FWA) was 3200 and 10900 ml/m<sup>2</sup>/day. So, the percentage increase in production in this case was 240% over the conventional SS.
4. The highest freshwater production was obtained for MSTSS-CA with PCMs-Ag-Nanos, where the combined productivity of the MSTSS-FWA with VCWSS and PCMs-Ag-NPs reached 11950 ml/m<sup>2</sup>/d, representing a substantial 273% increase over CSS.
5. The freshwater cost was \$0.028 per liter for CSS and \$0.011 per liter for modified stepped SS-FWA+VCWSS+PCMs-Ag.

#### Future Work

6. Future research directions could focus on improving and broadening the uses of the modified stepped solar still (MPSS). To assess the system's long-term robustness and effectiveness, extensive field testing in a variety of climates is necessary.
7. Thermal energy storage and release could be improved by adjusting PCMs properties during experiments with various materials and Nano concentration. Including renewable energy sources, like photovoltaic or solar thermal systems, can save operating costs and boost self-sufficiency.
8. It may be possible to get beyond the drawbacks of individual systems by investigating hybrid systems that integrate the MSTSS with additional desalination methods.

#### Study Limitations

Production difficulties include producing the fins, especially with large diameters, as well as manufacturing the steps, because it requires great precision to obtain good quality. Therefore, there is a manufacturing limit for the large dimensions of the stepped solar still, which depends on the manufacturing capabilities. We found that the process of charging the PCM under the steps requires high precision, due to the length of the steps. The PCM must be liquid, and the steps must be hot all the time so that voids do not occur inside the PCM as a result of its freezing.

#### References

- [1] UNESCO, WSSM. Water reuse within a circular economy context. 2nd ed. United Nations Educational: Scientific and Cultural Organization; 2020.
- [2] A.A. Saeed, A.M. Alharthi, K.M. Aldosari, A.S. Abdullah, F.A. Essa, U.F. Alqsair, M. Aljaghtham, Z.M. Omara, "Improving the drum solar still performance using corrugated drum and nano-based phase change material", *Energy Storage*. Vol. 55, 2022, 105647. <https://doi.org/10.1016/j.est.2022.105647>.
- [3] T. Taner, A Feasibility, "Study of Solar Energy-Techno Economic Analysis From Aksaray City, Turkey", *Thermal Engineering*, Vol. 3, No. 5, 2017, pp. 1-7. <https://doi.org/10.18186/journal-of-thermal-engineering.331756>.
- [4] F.A. Essa, M.A. Elaziz, M.A. Al-Betar, A.H. Elsheikh, "Performance prediction of a reverse osmosis unit using an optimized Long Short-term Memory model by hummingbird optimizer", *Process Safety and Environmental Protection*, Vol. 169, 2023, pp. 93–106. <https://doi.org/10.1016/j.psep.2022.10.071>.
- [5] F.A. Essa, M. Abd Elaziz, A.H. Elsheikh, "An enhanced productivity prediction model of active solar still using artificial neural network and Harris Hawks optimizer", *Appl. Therm. Eng.* 170 (2020) 115020. <https://doi.org/10.1016/j.applthermaleng.2020.115020>.
- [6] A.S. Abdullah, Z.M. Omara, F.A. Essa, M.M. Younes, S. Shanmugan, M. Abdelgaied, M.I. Amro, A.E. Kabeel, W.M. Farouk, "Improving the performance of trays solar still using wick corrugated absorber, nano-enhanced phase change material and photovoltaics-powered heaters", *Energy Storage*, Vol. 40, 2021, 102782. <https://doi.org/10.1016/j.est.2021.102782>.
- [7] B. Saleh, F.A. Essa, A. Aly, M. Alsehlhi, H. Panchal, A. Afzal, S. Shanmugan, "Investigating the performance of dish solar distiller with phase change material mixed with Al<sub>2</sub>O<sub>3</sub> nanoparticles under different water depths", *Environmental Science and Pollution Research*, Vol. 9, 2022, pp. 28115–28126. <https://doi.org/10.1007/s11356-021-18295-4>.
- [8] F.A. Essa, Z.M. Omara, A.S. Abdullah, S. Shanmugan, H. Panchal, A.E. Kabeel, R. Sathyamurthy, W.H. Alawee, A.M. Manokar, A.H. Elsheikh, "Wall-suspended trays inside stepped distiller with Al<sub>2</sub>O<sub>3</sub>/paraffin wax mixture and vapor suction: Experimental implementation", *Energy Storage*. Vol. 32, 2020, 102008. <https://doi.org/10.1016/j.est.2020.102008>.
- [9] Z.M. Omara, A.S. Abdullah, F.A. Essa, M.M. Younes, "Performance evaluation of a vertical rotating wick solar still", *Process Safety and Environmental Protection*, Vol. 148, 2021, pp. 796–804. <https://doi.org/10.1016/j.psep.2021.02.004>.
- [10] F.A. Essa, W.H. Alawee, S.A. Mohammed, H.A. Dhahad, A.S. Abdullah, Z.M. Omara, "Experimental investigation of convex tubular solar still performance using wick and nanocomposites", *Case Studies in Thermal Engineering*, Vol. 27, 2021, 101368. <https://doi.org/10.1016/j.csite.2021.101368>.
- [11] M.E.H. Attia, A.E. Kabeel, M. Abdelgaied, F.A. Essa, Z.M. Omara, "Enhancement of hemispherical solar still productivity using iron, zinc and copper trays", *Solar Energy*, Vol. 216, 2021, pp. 295–302. <https://doi.org/10.1016/j.solener.2021.01.038>.
- [12] Z.M. Omara, W.H. Alawee, S.A. Mohammed, H.A. Dhahad, A.S. Abdullah, F.A. Essa, "Experimental study on the performance of pyramid solar still with novel convex and dish absorbers and wick materials", *Cleaner Production*, Vol. 373, 2022, 133835. <https://doi.org/10.1016/j.jclepro.2022.133835>.
- [13] Y.A.F. El-Samadony, A.S. Abdullah, Z.M. Omara, "Experimental study of stepped solar still integrated with reflectors and external condenser", *Experimental Heat Transfer*, Vol. 28, 2015, pp. 392–404. <https://doi.org/10.1080/08916152.2014.890964>.

- [14] A.S. Abdullah, Z.M. Omara, A. Alarjani, F.A. Essa, "Experimental investigation of a new design of drum solar still with reflectors under different conditions", *case studies in thermal engineering*, Vol. 24, 2021, 100850. <https://doi.org/10.1016/j.csite.2021.100850>.
- [15] X. Zhang, Y., Zhao, X., Chen, Y., Chen, J., Yang, S., & Wang, "Design and performance of an inclined stepped solar still for seawater desalination", *Desalination*, Vol. 522, 2022, 115784.
- [16] A.M. Lashgari, S., Rostami, S., & Nikbakht, "Investigation of the effect of step number and inclination angle on the performance of a stepped solar still", *Desalination*, Vol. 506, 2021, 114981.
- [17] R.T. Ali, A. A., Al-Abodi, Y. A. J., & Al-Shamma'a, "Performance evaluation of a stepped solar still under local climatic conditions", *Desalination and Water Treatment*, Vol. 223, 2021, pp. 406–415.
- [18] M.T. Ahmed, M., Raza, S. M., & Sultan, "Comparative performance analysis of single and double slope stepped solar stills with and without PCM", *Renewable Energy*, Vol. 187, 2022, pp. 1193–1203.
- [19] M.S. El-Sebaey, A. Hegazy, F.A. Essa, "Performance enhancement of a tubular solar still by using stepped basins: An experimental approach", *Cleaner Production*, Vol. 437, 2024, 140746. <https://doi.org/10.1016/j.jclepro.2024.140746>.
- [20] K. Muafag Suleiman Tarawneh, "Effect of Water Depth on the Performance Evaluation of Solar Still", *Jordan Journal of Mechanical and Industrial Engineering*, Vol. 1, No. 1, 2007, pp. 23 – 29.
- [21] Imane Tronnebati, Fouad jawab, "Green and Sustainable Supply Chain Management: A Comparative Literature Review", *Jordan Journal of Mechanical and Industrial Engineering*, Vol. 17, No. 1, 2023, pp 115-126
- [22] M. J. A. A. S. M. P. A. M. a. M. E. H. A. Ehsan Abbasi Teshnizia, "Comprehensive Energy-Econo-Enviro (3E) Analysis of Grid Connected Household Scale Wind Turbines in Qatar", *Jordan Journal of Mechanical and Industrial Engineering*, Vol. 15, No. 12, 2021, pp. 215 - 231.
- [23] E. Azizi, Z. Khalili, M. Sheikholeslami. Simulation of solar photovoltaic system integrated with TEG in presence of hybrid nanomaterial. *Thermal Analysis and Calorimetry*, Vol. 149, 2024, PP. 5771–5782. <https://doi.org/10.1007/s10973-024-13192-7>.
- [24] Anandkushwah, Abdheshkumar, M. K. Gaur. Techno-economic analysis of solar still with nano-phase change material and heating coil: A novel approach for sustainable development. *Thermal Engineering*, Vol. 11, No. 2, 2025, pp. 476–492.
- [25] Holman J.P. *Experimental methods for engineers*, 8th ed. New York: McGraw-Hill Companies; 2011.
- [26] O. Bait, "Exergy, environ-economic and economic analyses of a tubular solar water heater assisted solar still", *Cleaner Production*, Vol. 212, 2019, pp. 630–646. <https://doi.org/10.1016/j.jclepro.2018.12.015>.